Biogeosciences Discuss., https://doi.org/10.5194/bg-2017-451
Manuscript under review for journal Biogeosciences
Discussion started: 10 November 2017
© Author(s) 2017. CC BY 4.0 License.

Biogeosciences Discussions
Open Access
EGU

Long-term response of oceanic carbon uptake to global warming via physical and biological pumps

Akitomo Yamamoto[1,2], Ayako Abe-Ouchi[1,2], Yasuhiro Yamanaka[3]

[1] Atmospheric an Ocean Research Institute, University of Tokyo, Kashiwa, Japan
[2]Japan Agency for Marine-Earth Science and Technology, Yokohama, Japan
[3]Graduate School of Environmental Science, Hokkaido University, Sapporo, Japan

Correspondence to: A. Yamamoto (akitomo@jamstec.go.jp)

Abstract. Global warming is expected to significantly decrease oceanic carbon uptake and therefore accelerate an increase in atmospheric CO_2 and global warming. The primary reasons in previous studies for the change in the oceanic carbon uptake are the solubility reduction due to seawater warming and changes in the ocean circulation and biological pump. However, quantifications of the contributions from different processes to the overall reduction in ocean uptake are still unclear. Herein, we investigate multimillennium response of oceanic carbon uptake to global warming and quantify the contributions of the physical and biological pump to the response using an atmosphere–ocean general circulation model and a biogeochemical model. We found that global warming reduced oceanic CO_2 uptake by 13% (30%) in the first 140 years (at year 2000), which is consistent with previous studies. Sensitivity studies show that changes in the biological pump via ocean circulation change and solubility change due to seawater warming are dominant processes in the uptake reduction. These results are contrary to most previous studies wherein circulation changes and solubility change from seawater warming are the dominant processes. The weakening of biological production and carbon export induced by lower nutrient supply diminishes the vertical gradient of DIC substantially reducing the CO_2 uptake. The weaker deep-ocean circulation decreases the downward transport of CO_2 from the surface to the deep ocean, leading to a drop in the CO_2 uptake in high-latitude regions. Conversely, weaker equatorial upwelling reduces the upward transport of natural CO_2 and therefore enhances the CO_2 uptake in low-latitude regions. Because these effects cancel each other, the circulation change becomes a second-order process. Our results suggest that the biological pump plays a significant role in the future oceanic carbon uptake through natural carbon cycle.

Biogeosciences Discuss., https://doi.org/10.5194/bg-2017-451
Manuscript under review for journal Biogeosciences
Discussion started: 10 November 2017
© Author(s) 2017. CC BY 4.0 License.

1 Introduction

By taking up approximately one-quarter of the anthropogenic CO_2 emissions since the beginning of the industrial era, the oceans have reduced the atmospheric CO_2 concentration and mitigated climate change (Ciais et al., 2014). In contrast to land uptake, oceanic carbon uptake operates over a 1000-year period (Plattner et al., 2008; Archer et al., 2009a; Zickfeld et al., 2013). Therefore, understanding changes in the ocean carbon cycle is crucial for predicting the long-term evolution of climate systems with slow response times, such as ice sheets (Charbit et al., 2008), permafrost (Lawrence and Slater, 2005), and methane hydrate in continental margins (Archer et al., 2009b; Yamamoto et al., 2014) as well as the atmospheric CO_2 concentration.

Climate warming tends to reduce the oceanic uptake of CO_2 from the atmosphere, thereby accelerating the rate of CO_2 accumulation in the atmosphere and global warming, which is well known as a positive climate–carbon cycle feedback (Cox et al., 2000; Dufresne et al., 2002; Friedlingstein et al., 2006). Changes in CO_2 solubility due to seawater warming, ocean circulation, and biological pump primarily alter the oceanic CO_2 uptake by affecting the anthropogenic CO_2 uptake and altering the air–sea balance of the natural CO_2 cycle. Most previous studies have shown that solubility change from seawater warming and circulation change are major contributors to the reduction in oceanic carbon uptake (Maier-Reimer et al., 1996; Sarmiento et al., 1998; Joos et al., 1999; Matear and Hirst, 1999; Plattner et al., 2001; Matsumoto et al., 2010). In those previous studies, changes in the biological pump associated with ocean circulation change were regarded as a second-order process even though biological pump has a crucial role in the natural carbon cycle.

On the other hand, changes in the biological pump can potentially contribute significantly to the reduction of the oceanic carbon uptake, considering that the previous and current generations of Earth system models (ESMs) show a consistent decrease in global mean export production between −6% and −20% by the year 2100 under strong climate warming (Steinacher et al., 2010; Bopp et al., 2013). A significant reduction in CO_2 uptake associated with the weakening of the biological pump was found in Zickfeld et al. (2008) even though they investigated the effect of just AMOC weakening caused by freshwater input. However, the contributions of both physical and biological effects to the reduction in oceanic CO_2 uptake are not evaluated directly in the recent generation of coupled atmosphere–ocean general circulation models (AOGCMs) and ocean biogeochemical models. To address this we examine the contribution of individual mechanisms to the changes in oceanic carbon uptake using a series of global warming simulation conducted with AOGCM and an offline ocean biogeochemical model. The methods applied here enable us to conduct multiple simulations of the ocean carbon cycle according to AOGCM climate simulations with low computational cost.

Previous studies using Earth System Models of Intermediate Complexity (EMICs) show that global warming decreases oceanic CO_2 uptake continuously over a thousand years or more (Plattner et al., 2008; Schmittner et al., 2008; Archer et al.,

© Author(s) 2017. CC BY 4.0 License.

2009a). These millennial-scale simulations are now feasible with atmosphere–ocean general circulation models (AOGCMs) due to increased computer power. Therefore, we conducted multi-millennium global warming simulations and sensitivity experiments using AOGCM and an offline ocean biogeochemical model. The second purpose of this study is to investigate the usefulness of EMIC for long-term simulations of the ocean carbon cycle by comparing our results to previous studies.

The remainder of the paper is organized as follows. Section 2 contains an introduction of the model and experiment design. Section 3 contains a description of the centennial- and millennial-scale changes in the climate and the ocean carbon cycle. We compare our model results to previous studies using ESMs and EMICs. In Section 4, we show the results of two sets of sensitivity studies and quantify the contribution of individual mechanisms to the reduction of the oceanic CO_2 uptake. A summary and discussion are provided in Section 5.

2 Methods

2.1 Climate model

We use the global-warming experiments conducted by Yamamoto et al (2015) with MIROC 4m AOGCM. This model is based on MIROC 3.2 (K-1 model developers, 2004). The MIROC 3.2 contributed to the Coupled Model Intercomparison Project phase 3 (Meehl et al., 2007), which was extensively cited in the Intergovernmental Panel on Climate Change Fourth Assessment Report. The coefficient of the isopycnal layer thickness diffusivity was 7.0×10^{-6} cm^2 s^{-1} instead of the value of 3.0×10^{-6} cm^2 s^{-1} used in the original MIROC 3.2. The atmospheric GCM has a horizontal resolution of T42 (~2.8°) and 20 vertical levels. The oceanic GCM has a zonal resolution of 1.4° and a spatially varying meridional resolution that is approximately 0.56° at latitudes lower than 8° and 1.4° at latitudes higher than 65°: the resolution changes smoothly between these latitudes. The vertical coordinate is a hybrid of sigma-z, resolving 44 levels in total: 8 sigma-layers near the surface, 35 z-layers beneath, and one bottom boundary layer (Nakano and Suginohara, 2002). The sea-ice component is based on a two-category thickness representation, zero-layer thermodynamics (Semtner, 1976), and dynamics using elastic–viscous–plastic rheology (Hunke and Dukowicz, 1997). A model spin-up has been performed under pre-industrial boundary conditions such as insolation and an atmospheric CO_2 concentration of 285 ppm.

2.2 Offline ocean biogeochemical model

The ocean carbon cycle is calculated by the MIROC-based offline biogeochemical model (Yamamoto et al., 2015). The offline biogeochemical model enables us to conduct numerous sensitivity experiments of the ocean carbon cycle according to AOGCM climate simulations with low computational cost. The horizontal and vertical resolution are the same as those of MIROC 3.2. For the tracer calculation, the monthly output data of velocity, temperature, salinity, sea surface height, sea-surface wind speed, sea-ice fraction, and sea-surface solar radiation from MIROC are applied to an offline tracer scheme (Oka et al., 2011). The biogeochemical model is a modified version of the nutrient–phytoplankton–zooplankton–detritus

© Author(s) 2017. CC BY 4.0 License.

(NPZD) ecosystem model of Keller et al. (2012). The model includes two phytoplankton classes (nitrogen fixers and other phytoplankton), zooplankton, particulate detritus, nitrate (NO_3), phosphate (PO_4), dissolved oxygen (O_2), dissolved inorganic carbon (DIC), alkalinity (ALK), two carbon isotopes (^{13}C and ^{14}C), and an ideal age tracer. Constant stoichiometry relates the C, N, and P content of the biological variables and their exchanges to the inorganic variables (NO_3, PO_4, O_2, ALK, and DIC). Optimal uptake kinetics, which assumes a physiological trade-off between the efficiency of nutrient encounter at the cell surface and the maximum assimilation rate (Smith et al., 2009), are adopted for the nutrient limitation of the growth rate of phytoplankton. The maximum phytoplankton growth and microbial remineralization rates are assumed to increase with seawater temperature according to Eppley (1972). The formulations of air–sea gas exchange and carbon chemistry follow the protocols of the Ocean Carbon Cycle Model Intercomparison Project–Phase 2 (OCMIP2; http://www.ipsl.jussieu.fr/OCMIP/phase2/) (Najjar and Orr, 1999). The production rate of calcium carbonate ($CaCO_3$) is assumed to be proportional to that of particulate organic carbon (POC, $CaCO_3$:POC = 0.03) and the setting flux of particulate $CaCO_3$ in the water column decreases with an e-folding depth of 3500 m (Schmittner et al., 2008). Although iron cycling is not explicitly calculated in our model, we adopt the iron limitation for the phytoplankton growth rate using monthly dissolved iron concentration outputs from pre-industrial experiments conducted using the biogeochemical elemental cycling model (AOU_06 case in Misumi et al., (2013)). Thus, we cannot consider changes in iron cycling and their impact on ecosystems in the global-warming experiment. We confirmed the validity of the offline calculation by comparing the salinity distribution calculated by the online and offline simulations. There were no significant differences between the two simulations.

The biogeochemical model is initialized from the annual mean climatology based on the World Ocean Atlas 2005 (WOA2005: Garcia et al., 2006) for dissolved NO_3 and PO_4 and Global Ocean Data Analysis Project (GLODAP: Key et al., 2004) for DIC and ALK. As for spin-up, the last 50 years of data in the MIROC pre-industrial experiment are cyclically applied to the offline ocean biogeochemical model. A model spin-up of more than 8000 years has been performed in order to eliminate the model drift in the global inventory of all tracers. In the last century of the spin-up run, the global net atmosphere–ocean CO_2 exchange is 3.0×10^{-4} PgC year^{-1}, which is smaller than the OCMIP2 threshold of 0.01 PgC year^{-1} (Orr, 2002). The resultant initial storage of ocean carbon (35,400 PgC), ocean net primary production (49.6 PgC year^{-1}) and export production (8.1 PgC year^{-1}) are comparable to observations and other estimates (Antoine et al., 1996; Schlitzer, 2000; Ciais et al., 2014). The simulated basin-scale distributions of nutrients (PO_4 and NO_3), DIC, and ALK are generally in agreement with the WOA2005 and GLODAP datasets (Fig. S1). All physical and biogeochemical tracers, except salinity, have correlation coefficients with the observations of more than 0.85 and normalized standard deviation values between 0.7 and 1.1 (Fig. S2).

Biogeosciences Discuss., https://doi.org/10.5194/bg-2017-451
Manuscript under review for journal Biogeosciences
Discussion started: 10 November 2017
© Author(s) 2017. CC BY 4.0 License.

2.3 Experimental design

After the spin-up, the prescribed atmospheric CO_2 concentration for the climate model was increased by 1% per year from the pre-industrial value (285 ppm) until it reached 4 × CO_2 levels (1140 ppm) at year 140. This value was then held constant until reaching 2000 years. Using the output of the global warming experiment conducted by the climate model, the offline biogeochemical model was integrated for 2000 years (GW in Table 1). This model does not include a marine-sediment module. The reaction of the dissolved CO_2 with $CaCO_3$ in deep ocean-sediments plays an important role only on longer timescales (Archer et al., 1998).

We conducted additional experiments using an offline biogeochemical model (Table 1). In the constant-climate run (CTL), the same prescribed CO_2 concentration as that used in GW but with the climate conditions of the MIROC pre-industrial experiment were applied to the offline biogeochemical model. The concept of this experiment is the same as the uncoupled simulation by Friedlingstein et al. (2006) wherein changing atmospheric CO_2 concentrations did not affect the radiation balance and therefore the climate. The total change in oceanic CO_2 uptake due to global warming is obtained from the difference between GW and CTL ("Total" in Table 2).

To isolate the sensitivity of CO_2 uptake with respect to changes in SST, ocean circulation, biology, freshwater flux, and sea ice, we conducted two sets of sensitivity experiments (Table 1). The first set of sensitivity experiments (GW-base) is based on Zickfeld et al. (2008). The experiments are based on GW; however, each mechanism is replaced from GW to CTL (3–9 in Table 1). The contributions of individual mechanisms to the CO_2 uptake change are calculated from the difference between GW and each experiment ("GW-base" in Table 2). Experiment GW_SST is identical to GW, except that pre-industrial SST is used to calculate the solubility. This experiment evaluates the influence of the solubility change due to the SST increase on the CO_2 uptake. Experiment GW_circ is based on GW; however, it uses the preindustrial ocean's vertical and horizontal velocities, sea surface height, vertical diffusivity, and oceanic interior temperature and salinity. Note that the archived monthly mean data of the source and sink of DIC and alkalinity due to the biological pump (the organic matter cycle and the $CaCO_3$ cycle) in GW are applied to the offline biogeochemical model. The CO_2 uptake sensitivity to ocean circulation change is isolated in this experiment. Experiments GW_om and GW_ca are similar to GW, except that the archived monthly mean data of the source and sink of DIC and alkalinity due to the organic matter and $CaCO_3$ cycles in CTL are applied to the offline biogeochemical model. These experiments evaluate the contributions of changes in the organic matter and $CaCO_3$ cycles. The biological effect is obtained from the sum of these two effects. Note that changes in productivity due to stratification and circulation change are included in not circulation effect but this biological effect. GW_si is similar to GW, except that the preindustrial sea ice fractions in both hemispheres are used. Note that this experiment isolates the effect of the gas exchange induced by the sea ice extent but does not include the effects of biological and circulation changes due to the sea ice coverage. GW_fw is identical to GW, except that the freshwater flux of the pre-industrial experiment is applied to the

Biogeosciences Discuss., https://doi.org/10.5194/bg-2017-451
Manuscript under review for journal Biogeosciences
Discussion started: 10 November 2017
© Author(s) 2017. CC BY 4.0 License.

offline biogeochemical model. This experiment evaluates the influence of changes in salinity, DIC, and alkalinity due to the hydrological cycle change on the CO_2 uptake.

The contributions of individual mechanisms to the CO_2 uptake change are also estimated from sensitivity experiments under pre-industrial climate conditions. In the second set (CTL-base), following GW-base, sensitivity experiments are based on CTL; however, each mechanism is replaced from CTL to GW (10–16 in Table 1). The contributions of individual mechanisms are obtained from the differences between each experiment and CTL ("CTL-base" in Table 2). The differences in the estimated contributions between GW-base and CTL-base are likely to reflect the non-linearity of each mechanism to the CO_2 uptake change.

3 Multi-millennium responses to global warming

3.1 Climate and ocean biogeochemical cycles

In this section, we briefly describe the regional changes in climate and ocean biogeochemical variables after the summary of the global mean changes reported in Yamamoto et al. (2015). At the end of the global warming simulation, the global mean surface air and ocean temperature increase by 8.4°C and 6.5°C, respectively. The AMOC decreases from 16.5 Sv to 3.8 Sv in the first 500 years and does not recover by the end of the simulation. The strength of the Antarctic Bottom Water (AABW) formation decreases from 6.2 Sv to 2.4 Sv in the first 500 years. Thereafter, the strength of the AABW formation recovers and overshoots the pre-industrial condition after year 1000. These global mean changes are comparable to previous long-term simulations with EMIC and AOGCM (see Yamamoto et al. (2015) for a more detailed discussion).

At the time of CO_2 quadrupling (year 140), polar amplification occurs only in the Northern Hemisphere (Fig. 1a). The surface temperature over the Southern Ocean and Antarctica gradually increases, and polar amplification in both hemispheres is observed at approximately year 1000. This slow southern polar warming is related to deep-ocean heat uptake in the Southern Ocean. According to the slow deep-ocean heat uptake, the ocean interior is still warming up at the end of the simulations (Fig. 1b). Slow southern polar warming and ocean heat uptake have also been reported in previous multi-millennial simulations conducted by ECHAM5/MPIOM (Li et al., 2013). In the ocean, greater warming of the upper ocean (above 2000 m) occurs in the Southern Hemisphere (Fig. 1c). This is because the drastically weakened AMOC and enhanced AABW formations cause the heat transport to be larger in the Southern Hemisphere than in the Northern Hemisphere (Fig. 1d). Weakening in AMOC reduces the heat transport from 1.8 PW to 0.8 PW across 30° N. By contrast, enhanced AABW increases heat transport by 0.7 PW in the Southern Hemisphere.

Strengthening and poleward shifting of the subpolar westerlies occurs in the Southern Hemisphere (Figure 1e), which is consistent with the observations and a robust feature of climate projections in global-warming experiments (Fyfe and Saenko,

Biogeosciences Discuss., https://doi.org/10.5194/bg-2017-451
Manuscript under review for journal Biogeosciences
Discussion started: 10 November 2017
© Author(s) 2017. CC BY 4.0 License.

2006; Meijers, 2014). A 12% strengthening and a 2.8° poleward shift of the maximum annual mean zonal wind stress occur at the time of CO_2 quadrupling. Subsequently, the subpolar westerlies in the Southern Hemisphere are gradually weakened but are still slightly stronger than the pre-industrial conditions. This weakening occurs because the slow southern polar warming weakens the thermal gradient between the tropical and polar areas. The contributions of ocean-circulation change caused by strengthened westerlies to the ocean carbon cycle are discussed in Section 4.2.

Global PO_4 concentration at the surface decreases by about 25%. This decrease is attributed to reduced nutrient supply into the euphotic zone due to enhanced stratification and slower deep-ocean circulation. As a result, the global export production decreases by 22% (see fig. 1d in Yamamoto et al., 2015), which is comparable with CMIP5 models (7%-18% reduction in export production from 1990s to 2090s for RCP8.5) (Bopp et al., 2013). Remarkable reduction in surface PO_4 concentration occurs in the tropical ocean and the North Atlantic (Fig. 1f). According to surface PO_4 reduction, the largest declines in export production are also located around the equator and in the North Atlantic (Fig. 1g). The increases in export production are primarily observed in the Southern and Arctic Oceans. These increases are related to reductions in light limitation and/or increased growth rates due to rising temperatures as shown by Steinacher et al. (2010).

Due to the constant production ratio of POC and $CaCO_3$ in the model formulation and the increase in the global primary production by 2.5 PgC $year^{-1}$ from the preindustrial value, $CaCO_3$ production is increased by 6%. The export of $CaCO_3$ also increases in spite of a reduction in the POC export, resulting in the rain ratio increasing from 0.09 to 1.13. Two distinct export responses are caused by faster and shallower remineralization of POC in a warmer ocean; however, the remineralization rate of $CaCO_3$ is independent of the seawater temperature in our model. The enhanced $CaCO_3$ production decreases (increases) alkalinity in the surface (deep) oceans as shown by the changes in the salinity-normalized alkalinity (the dashed lines in Fig. 1h). The surface alkalinity reduction is also caused by the longer residence time of the surface waters, which allow a more efficient biological utilization of the carbonate ions. The enhanced surface-to-deep gradient of the salinity-normalized alkalinity and the alkalinity associated with changes in the $CaCO_3$ cycling and ocean circulation has been reported in previous long-term simulations (Plattner et al., 2001; Schmittner et al., 2008). Changes in the freshwater flux also alter the alkalinity. At low latitudes, enhanced evaporation concentrates the surface alkalinity. Dilution of the surface alkalinity by enhanced precipitation at high latitudes reduces the alkalinity in the deep ocean. As a result, changes in the freshwater flux causes weaker surface-to-deep gradients of the alkalinity. The effects of changes in the $CaCO_3$ cycling and freshwater flux cancel each other out, resulting in apparently slight changes in the surface-to-deep gradient of alkalinity in our model (solid lines in Fig. 1h). The quantitative attribution of changes in the $CaCO_3$ cycle and freshwater flux to the CO_2 uptake change are discussed in Section 4.1.

Biogeosciences Discuss., https://doi.org/10.5194/bg-2017-451
Manuscript under review for journal Biogeosciences
Discussion started: 10 November 2017
© Author(s) 2017. CC BY 4.0 License.

3.2 Ocean carbon cycle

We first show the cumulative oceanic uptake of CO_2 and the reduction of oceanic CO_2 uptake due to global warming. At the time of CO_2 quadrupling (year 140), the cumulative CO_2 uptake is 567 PgC in the global warming run (GW). In comparison to the cumulative CO_2 uptake of 654 PgC in the constant climate run (CTL), the projected reduction in the cumulative CO_2 uptake due to global warming is 13%. These values are close to those of the same simulation using models in the Coupled Model Intercomparison Project 5 (CMIP5, (Taylor et al., 2012)); the model mean CO_2 uptake is 613 PgC and the uptake reduction is 11% (Arora et al., 2013). Even though oceanic CO_2 uptake is decreased during constant atmospheric CO_2, a new equilibrium is not yet reached by the end of the simulation. In the last decade of the experiments, the ocean still takes up approximately 0.31 PgC $year^{-1}$ due to the millennial timescale of the deep ocean ventilation (Key et al., 2004). At the end of the simulation, the cumulative CO_2 uptake is 2028 PgC and the uptake reduction due to global warming increases to 30% (Fig. 2a and Table 1). These values and the increasing trend of the uptake reduction are also comparable to the results of previous long-term simulations with EMIC (Plattner et al., 2001; Schmittner et al., 2008).

The time evolutions of oceanic CO_2 uptake in each basin are shown in Figure 2b. In the first few decades, the Pacific Ocean is the dominant sink of atmospheric CO_2 because it possesses the largest area. After atmospheric CO_2 stops increasing, the surface Pacific waters are close to saturation and CO_2 uptake rapidly decreases because the deep Pacific waters are slowly ventilated. Conversely, the decrease in CO_2 uptake in the Southern Oceans is slower than that in the Pacific Ocean. Carbon transport from the surface to deep ocean via the well-ventilated waters causes continuous CO_2 uptake there. In the pre-industrial condition, the pCO_2 in the Southern Ocean is kept higher than the atmospheric pCO_2 owing to the upwelling of carbon-rich deep waters, resulting in a source of atmospheric CO_2. The Southern Ocean alters from a source to a sink of atmospheric CO_2 immediately after the atmospheric CO_2 increase. This phenomenon is consistent with observation-based reconstructions of present-day and pre-industrial air–sea CO_2 fluxes (Gruber et al., 2009). After excess CO_2 is mixed throughout the deep ocean, the pCO_2 in the Southern Ocean again exceeds the atmospheric pCO_2. The Southern Ocean returns to being a source of atmospheric CO_2 at approximately year 1400. At the end of the global warming experiment, the Atlantic and Southern Oceans are the major sink and source basins of atmospheric CO_2, respectively, as in the pre-industrial condition.

Here, we investigate the regional differences of uptake reduction due to global warming. In the first 500 years, approximately half of the total uptake reduction occurs in tropical and subtropical regions between 32.5°S and 32.5°N (Fig. 2c). The contributions of the high latitudes in the Northern and Southern Hemispheres have similar magnitudes. At the basin scale, the contributions of the Atlantic and Pacific Ocean have similar magnitudes and that of the Indian Ocean is approximately half those contributions. These regional differences have also been found in similar long-term simulations by Plattner et al. (2001). The global and regional changes of the oceanic CO_2 uptake projected in this study using AOGCM and

© Author(s) 2017. CC BY 4.0 License.

the offline ocean biogeochemical model are comparable to previous long-term simulations with EMIC. Therefore, our results support the usefulness of EMIC for long-term projections of the ocean carbon cycle.

Figure 3 shows the zonal mean distribution of the salinity-normalized DIC (sDIC) in the global warming run. In the first 500 years, changes in sDIC from the pre-industrial condition decrease from the surface to deep oceans. Significant sDIC changes in the deep water are observed in the North Atlantic. The shallower CO_2 invasion into the North Atlantic compared to the constant climate run (Fig. S3) is caused by the weaker and shallower AMOC. After year 1000, due to the enhanced AABW formation, AABW with a relatively high sDIC concentration intrudes into the deep North Atlantic below 2000 m. As a result, the largest sDIC change in the deep water occurs in the North Atlantic at the end of the simulations. The smallest sDIC change is found in the deep North Pacific in accordance with the millennial ventilation timescale.

4 Effects of individual mechanisms on the reduction in oceanic CO2 uptake associated with global warming

The decrease in cumulative CO_2 uptake due to global warming projected in our model is consistent with the previous centennial and millennial simulations with ESMs and EMICs. In this section, we disentangle the contributions of individual mechanisms to CO_2 uptake reduction using two sets of sensitivity experiments (GW-base and CTL-base experiments). The conducted sensitivity experiments and the procedure to isolate each contribution are summarized in Tables 1 and 2. Averages of the GW-base and CTL-base experiments are used below. To compare our results with previous studies, we focus on changes in the CO_2 uptake in the first 500 years. The total reduction in the cumulative CO_2 uptake until year 500 is 402 PgC ("Total" in Table 2).

4.1 Global change

Changes in the organic matter cycle and the solubility due to the SST increase are the dominant mechanisms for the global reduction in the CO_2 uptake due to global warming (Fig. 4). At year 500, changes in the organic matter cycle and reduced solubility due to sea-surface warming decrease the global carbon uptake by 276 PgC and 151 PgC, respectively. A significant nonlinearity of the uptake change is found in the effect of the organic matter cycle (an uptake change from −216 PgC to −336 PgC). The ocean circulation change decreases the global CO_2 uptake by 6.5 PgC.

Enhanced $CaCO_3$ production reduces the surface alkalinity and therefore leads to an increase in the surface pCO_2. Changes in the $CaCO_3$ cycle reduce the CO_2 uptake by 14 PgC. The reduced sea ice cover allows air–sea gas exchange over a larger area and leads to an increase in the CO_2 uptake by 15 PgC. Dilution of the surface salinity by 1 psu leads to a pCO_2 reduction of approximately 4% (Takahashi et al., 1993) and an increase in the CO_2 uptake. Enhanced evaporation at low latitudes increases pCO_2 resulting in an uptake reduction, whereas enhanced precipitation at high latitudes increases uptake. The global contribution of changes in the freshwater flux is an uptake reduction of 2.5 PgC.

© Author(s) 2017. CC BY 4.0 License.

The significant contribution of changes in the organic matter cycle on the uptake reduction due to global warming and the secondary importance of the circulation change are consistent with Zickfield et al. (2008) in which the reduction in the oceanic CO_2 uptake due to freshwater hosing and AMOC weakening was investigated. However, these results are different from most previous global warming studies (Sarmiento et al., 1998; Joos et al., 1999; Matear and Hirst, 1999; Plattner et al., 2001; Matsumoto et al., 2010), in which ocean circulation was the dominant mechanisms for the reduction in oceanic CO_2 uptake. Below, we investigate what causes the greater biological effect and smaller circulation effect in our global warming simulations.

4.2 Effects of circulation change

The effects of circulation change display large regional variations (Fig. 4). Weaker AMOC and AABW formation decrease the downward transport of CO_2 from the surface to the deep ocean, leading to a drop in the CO_2 uptake at high latitudes and thus a reduction in sDIC in the deep ocean (Fig. 5). On the other hand, CO_2 uptake at low latitudes is enhanced by ocean circulation. This increase is attributed to weaker upper-ocean overturning and tropical upwelling (Fig. 6a). The tropical upwelling across 200m decreases from 38 Sv to 22.5 Sv in the first 200 years and continues to the end of the simulation (Fig. 6b). Weakening the equatorial upwelling reduces the upward transport of natural CO_2 from the ocean interior to the surface. The resulting enhanced CO_2 uptake at low latitudes increases sDIC in the subsurface water, especially in the Pacific Ocean (Fig. 5). The importance of enhanced CO_2 uptake associated with weaker upper-ocean overturning is also suggested in decadal variability of oceanic CO_2 uptake (DeVries et al., 2017).

An increase in sDIC also occurs in the Antarctic intermediate water. The intensification of the Southern Hemisphere westerly winds, as previously mentioned, enhances the mixing and overturning circulation of the Southern Ocean (Fig. 6a), increasing the CO_2 uptake and sDIC (Fig. 5). An enhanced CO_2 uptake due to intensified westerly wind in the Southern Ocean has also been observed in previous studies using simple box models and coupled general-circulation models (Zickfeld et al., 2007; Le Quéré et al., 2008; Matear and Lenton, 2008).

Enhanced CO_2 uptake induced by weaker equatorial upwelling and increased westerly wind cancel out the reduced CO_2 uptake associated with stratification and the weaker deep ocean circulation. Therefore, the effects of circulation change are responsible for a small fraction of the total reduction in the CO_2 uptake in our simulations. In the first 200 years, increases in CO_2 uptake caused by weaker equatorial upwelling and strengthened westerly winds are dominant processes in the effect of circulation change (Fig. 7). Subsequently, the effects of weaker AMOC and AABW formation are enhanced and overcome those of the strengthened westerly wind and weaker equatorial upwelling. As a result, the CO_2 uptake is reduced by the circulation change after year 450.

© Author(s) 2017. CC BY 4.0 License.

4.3 Effects of changes in the biological pump

Reduced nutrient supply into the euphotic zone due to circulation change and faster remineralization from seawater warming decrease the POC flux by 22% at a depth of 100m and 70% at a depth of 1000 m (Fig. 1e and 8a). The weaker carbon transport by the biological pump cannot maintain the vertical gradient of DIC between the surface and deep oceans. Excess DIC stored in the deep ocean by the biological pump is transported to the surface, therefore increasing surface pCO_2 and reducing CO_2 uptake. Reduced CO_2 uptake occurs at the low latitude and the high latitudes in the Northern Hemisphere (Fig. 4) according to changes in export production (Fig. 1g). Similarly, significant sDIC decreases occur in the North Atlantic, equatorial Indo-Pacific Ocean, and North Pacific (Fig. 8b). Reduction in CO_2 uptake induced by weaker biological pump are consistent with previous model simulations in which a significant atmospheric CO_2 increase is caused by a complete die-off of ocean life (Maier-Reimer et al., 1996; Sarmiento and Gruber, 2006).

Subsequently, the effect of the reorganization of the biological pump on the reduction in CO_2 uptake is decomposed into the effects of the temperature dependence of production and remineralization and the change in nutrient supply via the circulation change. The production and remineralization rate doubles for every 10°C increase in the seawater temperature in our model (Eppley, 1972). The warming-induced increase in production reduces the partial pressure of CO_2, therefore enhancing the oceanic CO_2 uptake. Enhanced remineralization of organic matter reduces the carbon transport into the deep ocean, leading to a lower CO_2 uptake. The lower nutrient supply due to stratification and slower thermohaline circulation decreases export production and therefore CO_2 uptake. The effect of the temperature dependence of the biological pump is calculated in GW-base and CTL-base ("Temperature for biology" in Table 2). The effect of the change in the nutrient supply is calculated as the residual ("Biology" − "Temperature for biology" as summarized in Table 2).

In the first 100 years, a warming-induced increase in production occurs more rapidly than an increase in remineralization because the surface waters are warming more rapidly than the subsurface. Therefore, the temperature dependence slightly increases the CO_2 uptake (Fig. 7). Subsequently, the effect of the enhanced remineralization overcomes that of the enhanced production and therefore the temperature dependence decreases the CO_2 uptake, which is consistent with the findings of Matsumoto (2007). At year 500, lower nutrient supply and temperature dependence decreases the CO_2 uptake by 241.5 PgC and 48.5 PgC, respectively (Table 2). Our results indicate that the reduction in the oceanic CO_2 uptake by biological change is mainly caused by reduction in nutrient supply via the circulation change, and temperature effects on production and remineralization are not negligible.

5 Summary and Discussion

In this study, we investigated multi-millennial changes in the ocean carbon cycle under a quadrupling of the atmospheric carbon dioxide using an AOGCM and an offline biogeochemical model. At the end of the simulation, the cumulative CO_2

© Author(s) 2017. CC BY 4.0 License.

uptake is 2028 PgC and global warming reduces the uptake by 30%. The reduction in the oceanic CO_2 uptake due to global warming primarily occurs in the tropical and subtropical regions. These global and regional changes in the oceanic CO_2 uptake projected in this study are similar to those in previous long-term simulations with EMIC (Plattenr et al., 2001; Schmittner et al., 2008). Our results support the usefulness of EMIC for long-term projections of the ocean carbon cycle.

To isolate and quantify the individual mechanisms that are responsible for the reduction in the oceanic CO_2 uptake due to global warming, we conducted two sets of sensitivity experiments based on Zickfeld et al. (2008). Our results show that changes in the organic matter cycle via ocean circulation change and reduced solubility due to sea surface warming are the primary contributors to the reduction in the CO_2 uptake due to global warming. For circulation changes, the effects of both the reduced upward transport of natural CO_2 and the reduced downward transport of anthropogenic CO_2 are represented. The reduced CO_2 uptake associated with weaker deep ocean circulation and stratification is counteracted by the enhanced uptake due to weaker equatorial upwelling and strengthened subpolar westerly winds in the Southern Hemisphere. Consequently, the circulation change is a second-order process. The weakening of the biological carbon export resulting from a lower nutrient supply and the enhanced remineralization owing to seawater warming diminishes the gradient of DIC between the surface and deep ocean, leading to a significant reduction in the oceanic CO_2 uptake. The circulation change reduces the global CO_2 uptake via changes in the biological pump rather than directly.

The significant contribution of changes in the organic matter cycle on the uptake reduction due to global warming and the secondary importance of the circulation change are consistent with Zickfield et al. (2008) in which the reduction in the oceanic CO_2 uptake due to freshwater hosing and AMOC weakening was investigated. However, these results are different from most of the previous global warming studies (Sarmiento et al., 1998; Joos et al., 1999; Matear and Hirst, 1999; Plattner et al., 2001; Matsumoto et al., 2010), in which ocean circulation was the dominant mechanisms for the reduction in oceanic CO_2 uptake. The important differences between most previous studies and this study are the resolution of climate model and complexity of biogeochemical model. Our model has an increased atmospheric and oceanic resolutions, so we hypothesise it captures better weaker equatorial upwelling and enhanced mixing due to strengthened subpolar westerly wind in the Southern Hemisphere. These physical changes are not reported in the previous studies. Therefore, the effect of circulation changes in our simulation would be smaller than in the previous studies. These physical changes also affect the nutrient supply and production. Moreover, the temperature dependence of production and remineralization was not considered in most of previous studies using simple ocean biogeochemical models (such as nutrient-restoring model). These mechanisms would lead to larger biological effects relative to previous studies.

The methods used to quantify the effect of ocean circulation on the changes in oceanic carbon uptake are also different between most previous studies and this study. In the former typical method (Sarmiento et al., 1998; Plattner et al., 2001; Matsumoto et al., 2010), abiotic experiments (i.e., without a biological pump) were conducted to isolate the physical process

© Author(s) 2017. CC BY 4.0 License.

from the biological process. In the abiotic experiments, the vertical gradient of DIC under the pre-industrial condition is much smaller than realistic vertical gradient of DIC because biological process primarily maintain most of the surface-to-deep gradient of DIC as shown in Sarmiento and Gruber (2006). The circulation effect estimated by the abiotic experiments would underestimate the enhanced CO_2 uptake associated with the reduced upward transport of natural CO_2 from the deep ocean to the upper ocean. The reduced CO_2 uptake due to the reduced downward transport of anthropogenic CO_2 from the surface to deep ocean are primarily represented. This study based on Zickfeld et al. (2008) separated these two effects more directly. In our methods (CTL-base/GW-base experiments) with a realistic vertical gradient of DIC, the effect of the circulation change represents both a reduced upward transport of natural CO_2 and a reduced downward transport of anthropogenic CO_2. Therefore, the contribution of circulation changes to the reduction in CO_2 uptake in the previous studies would be larger than that in this study.

Changes in the oceanic carbon uptake and reductions in the export production due to global warming are consistent with current simulations using ESMs. Therefore, we speculate that similar contributions of changes in ocean circulation and biological processes to the reduction in CO_2 uptake will be found in other models. To assess the robustness of our results for the reduction in oceanic CO_2 uptake due to global warming, analyses using other recent GCM and ocean biogeochemical models are required.

Our study shows that the change in the biological pump is crucial for the reduction in the oceanic CO_2 uptake due to global warming; however, there are several biological processes that are not considered in our model. The reduction in the saturation levels of calcium carbonate in seawater associated with CO_2 invasion into the ocean has adverse effects on marine calcifying organisms. The reduction in $CaCO_3$ production would increase the surface ocean alkalinity and therefore enhance the oceanic carbon uptake (Riebesell et al., 2000); however its impact has been very different in various previous modeling studies (Heinze, 2004; Gehlen et al., 2007; Ridgwell et al., 2007; Matsumoto et al., 2010). An increase in biotic carbon-to-nitrogen drawdown in response to pCO_2 changes enhances oceanic CO_2 uptake (Oschlies et al., 2008). Reduced seawater viscosity in a warmer ocean accelerates particle sinking speed, therefore increasing the efficiency of the biological pump and enhancing oceanic CO_2 uptake (Bach et al., 2012; Taucher et al., 2014). These effects remain poorly understood but could potentially have a large impact on oceanic carbon uptake and atmospheric CO_2 concentration on a multi-centennial to millennial timescale. The inclusion of these processes may be required for a comprehensive understanding of the response of the ocean carbon cycle to global warming.

Acknowledgements

Data are freely available upon request from the corresponding author (akitomo@jamstec.go.jp). This research was supported by the Environment Research and Technology Development Fund (S-10) of the Ministry of the Environment, Japan.

© Author(s) 2017. CC BY 4.0 License.

AOGCM simulations were carried out on the JAMSTEC Earth Simulator. The simulations with offline biogeochemical model were performed using the Fujitsu PRIMEHPC FX10 System in the Information Technology Center, University of Tokyo.

References

Antoine, D., André, J.-M., and Morel, A.: Oceanic primary production: 2. Estimation at global scale from satellite (coastal zone color scanner) chlorophyll, Global Biogeochem. Cycles, 10, 57–69, 1996.

Archer, D., Kheshi, H., and Maier-Reimer, E.: Dynamics of fossil fuel CO_2 neutralization by marine $CaCO_3$, Global Biogeochem. Cycles, 12, 259–276, 1998.

Archer, D., Eby, M., Brovken, V., Ridgwell, A., Cao, L., Mikolajewicz, U., Caldeira, K., Matsumoto, K., Munhoven, G., Montenegro, A., and Tokos, K.: Atmospheric lifetime of fossil fuel carbon dioxide, Annu. Rev. Earth Planet. Sci., 37, 117–134, 2009a.

Archer, D., Buffett, B., and Brovkin, V.: Ocean methane hydrates as a slow tipping point in the global carbon cycle, Proc. Natl. Acad. Sci. U.S.A., 106, 20,596–20,601, doi:10.1073/pnas.0800885105, 2009b.

Arora, V. K., Boer, G. J., Friedlingstein, P., Eby, M., Jones, C. D., Christian, J. R., Bonan, G., Bopp, L., Brovkin, V., Cadule, P., Hajima, T., Ilyina, T., Lindsay, K., Tjiputra, J. F., and Wu, T.: Carbon-concentration and carbon-climate feedbacks in CMIP5 Earth system models, J. Clim., 26(15), 5289–5314, doi:10.1175/jcli-d-12-00494.1, 2013.

Bach, L. T., Riebesell, U., Sett, S., Febiri, S., Rzepka, P., and Schulz, K. G.: An approach for particle sinking velocity measurements in the 3-400 µm size range and considerations on the effect of temperature on sinking rates, Mar. Biol., 159(8), 1853-1864, doi:10.1007/s00227-012-1945-2, 2012.

Bopp, L., Resplandy, L., Orr, J. C., Doney, S. C., Dunne, J. P., Gehlen, M., Halloran, P., Heinze, C., Ilyina, T., Séférian, R., Tjiputra, J., and Vichi, M.: Multiple stressors of ocean ecosystems in the 21st century: Projections with CMIP5 models, Biogeosciences, 10, 6225–6245, doi:10.5194/bg-10-6225-2013, 2013.

Charbit, S., Paillard, D., and Ramstein, G.: Amount of CO_2 emissions irreversibly leading to the total melting of Greenland, Geophys. Res. Lett., 35, L12503, doi:10.1029/2008GL033472, 2008.

Ciais, P., et al. : Carbon and other biogeochemical cycles, in Climate Change 2013: The Physical Science Basis. Contribution of Working Group I to the Fifth Assessment Report of the Intergovernmental Panel on Climate Change, edited by T. F. Stocker et al., pp. 465–570, Cambridge Univ. Press, Cambridge, U. K., and New York, 2014.

Ciais, P., Sabine, C., Bala, G., Bopp, L., Brovkin, V., Canadell, J., Chhabra, A., DeFries, R., Galloway, J., Heimann, M., Jones, C., Le Quéré, C., Myneni, R. B., Piao, S., and Thornton, P.: Carbon and Other Biogeochemical Cycles, in: Climate Change 2013: The Physical Science Basis. Contribution of Working Group I to the Fifth Assessment Report of the Intergovernmental Panel on Climate Change, edited by: Stocker, T. F., Qin, D., Plattner, G.-K., Tignor, M.,

© Author(s) 2017. CC BY 4.0 License.

Allen, S. K., Boschung, J., Nauels, A., Xia, Y., Bex, V., and Midgley, P. M., Cambridge University Press, Cambridge, United Kingdom and New York, NY, USA, 465– 570, 2013.

Cox, P. M., Betts, R. A., Jones, C. D., Spall, S. A., and Totterdell, I. J.: Acceleration of global warming due to carbon-cycle feedbacks in a coupled climate model, Nature, 408(6809), 184–187, 2000.

DeVries, T., Holzer, M., and Primeau, F.: Recent increase in oceanic carbon uptake driven by weaker upper-ocean overturning, Nature, 542, 215–218. doi:10.1038/nature21068, 2017

Dufresne, J. L., Friedlingstein, P., Berthelot, M., Bopp, L., Ciais, P., Fairhead, L., Treut, H. L., and Monfray, P.: On the magnitude of positive feedback between future climate change and the carbon cycle, Geophys. Res. Lett., 29(10), 1405, doi:10.1029/2001GL013777, 2002.

Eppley, R. W.: Temperature and phytoplankton growth in the sea, Fish. Bull., 70, 1063–1085, 1972.

Friedlingstein, P., Cox, P., Betts, R., Bopp, L., von Bloh, W., Brovkin, V., Cadule, P., Doney, S., Eby, M., Fung, I., Bala, G., John, J., Jones, C., Joos, F., Kato, T., Kawamiya, M., Knorr, W., Lindsay, K., Matthews, H. D., Raddatz, T., Rayner, P., Re- ick, C., Roeckner, E., Schnitzler, K.-G., Schnur, R., Strassmann, K., Weaver, A. J., Yoshikawa, C., and Zeng, N.: Climate–Carbon Cycle Feedback Analysis: Results from the C4MIP Model Inter- comparison, J. Clim. 19, 3337–3353, doi:10.1175/JCLI3800.1, 2006.

Fyfe, J. C., and Saenko, O. A.: Simulated changes in the extratropical Southern Hemisphere winds and currents, Geophys. Res. Lett., 33, L06701, doi:10.1029/2005GL025332, 2006.

Garcia, H. E., Locarnini, R. A., Boyer, T. P., and Antonov, J. I.: World Ocean Atlas 2005, Vol. 4, Nutrients (Phosphate, Nitrate, Silicate), NOAA Atlas NESDIS, vol. 64, edited by S. Levitus, 396 pp., U.S. Gov. Print. Off., Washington, D. C, 2006.

Gehlen, M., Gangst, R., Schneider, B., Bopp, L., Aumont, O., and Ethe, C.: The fate of pelagic $CaCO_3$ production in a high CO_2 ocean: A model study, Biogeosciences, 4, 505–519, 2007.

Gruber, N., Gloor, M., Fletcher, S. E. M., Doney, S. C., Dutkiewicz, S., Follows, M. J., Gerber, M., Jacobson, A. R., Joos, F., Lindsay, K., Menemenlis, D., Mouchet, A., Muller, S. A., Sarmiento, J. L., and Takahashi, T.: Oceanic sources, sinks, and transport of atmospheric CO2, Global Biogeochem. Cy., 23, GB1005, doi:10.1029/2008gb003349, 2009.

Heinze, C.: Simulating oceanic $CaCO_3$ export production in the greenhouse, Geophys. Res. Lett., 31, L16308, doi:10.1029/2004GL026013, 2004.

Hunke, E. C., and Dukowicz, J. K.: An elastic-viscous-plastic model for sea ice dynamics, J. Phys. Oceanogr., 27(9), 1849–1867, doi:10.1175/1520-0485(1997)027<1849:AEVPMF>2.0.CO;2, 1997.

Joos, F., Plattner, G. K., Stocker, T. F., Marchal, O., and Schmittner, A.: Global warming and marine carbon cycle feedbacks on future atmospheric CO_2, Science, 284(5413), 464– 467, 1999.

K-1Model Developers: K-1 Coupled GCM (MIROC) description, editedbyH. Hasumi, and S.Emori, K-1 Tech. Rep. 1, 34pp., Univ.of Tokyo, Tokyo, 2004.

© Author(s) 2017. CC BY 4.0 License.

Keller, D. P., Oschlies, A., and Eby, M.: A new marine ecosystem model for the University of Victoria Earth System Climate Model, Geosci. Model Dev., 5(5), 1195–1220, doi:10.5194/gmd-5-1195-2012, 2012.

Key, R. M., Kozyr, A., Sabine, C. L., Lee, K., Wanninkhof, R., Bullister, J. L., Feely, R. A., Millero, F. J., Mordy, C., and Peng, T.-H.: A global ocean carbon climatology: Results from Global Data Analysis Project (GLODAP), Global Biogeochem. Cycles, 18, GB4031, doi:10.1029/2004GB002247, 2004.

Lawrence, D. M., and Slater, A. G.: A projection of severe near-surface permafrost degradation during the 21st century, Geophys. Res. Lett., 32 L24401, doi:10.1029/2005GL025080, 2005.

Le Quéré, C., Rödenbeck, C., Buitenhuis, E. T., Conway, T. J., Langenfelds, R., Gomez, A., Labuschagne, C., Ramonet, M., Nakazawa, T., Metzl, N., Gillett, N. P., and Heimann, M.: Response to Comments on ‘‘Saturation of the Southern Ocean CO_2 sink due to recent climate change’’. Science 319, 570, 2008.

Li, C., von Storch, J.-S., and Marotzke, J.: Deep-ocean heat uptake and equilibrium climate response, Clim. Dyn., 40, 1071–1086, doi:10.1007/s00382-012-1350-z, 2013.

Maier-Reimer, E., Mikolajewicz, U., and Winguth, A.: Future ocean uptake of CO_2: Interaction between ocean circulation and biology, Clim. Dyn., 12(10), 711– 721, 1996.

Matear, R., and Hirst, A.: Climate change feedback on the future oceanic CO_2 uptake, Tellus, 51B, 722– 733, 1999.

Matear, R. J., and Lenton, A.: Impact of historical climate change on the Southern Ocean carbon cycle, J. Clim., 21, 5820–5834, 2008.

Matsumoto, K.: Biology-mediated temperature control on atmospheric pCO_2 and ocean biogeochemistry, Geophys. Res. Lett., 34, L20605, doi:10.1029/2007GL031301, 2007.

Matsumoto, K., Tokos, K., Chikamoto, M. O., and Ridgwell, A.: Characterizing post-industrial changes in the ocean carbon cycle in an Earth system model, Tellus Ser. B, 62, 296–313, 2010.

Meehl, G. A., Stocker, T. F., Collins,W. D., Friedlingstein, P., Gaye, A. T., Gregory, J. M., Kitoh, A., Knutti, R., Murphy, J. M., Noda, A., Raper, S. C. B.,Watterson, I. G.,Weaver, A. J., and Zhao, Z.-C.: Climate Change 2007: The Physical Science Basis. Contribution of Working Group I to the Fourth Assessment Report of the Intergovernmental Panel on Climate Change, chap. Global Climate Projections, 747–846, Cambridge University Press, Cambridge, United Kingdom and New York, NY, USA, 2007.

Meijers, A.: The Southern Ocean in the Coupled Model Intercomparison Project phase 5, Philos. Trans. R. Soc. A, 372(2019), 20130,296, doi:10.1098/rsta.2013.0296, 2014.

Misumi, K., Lindsay, K., Moore, J. K., Doney, S. C., Tsumune, D., and Yoshida, Y.: Humic substances may control dissolved iron distributions in the global ocean: Implications from numerical simulations, Global Biogeochem. Cycles, 27, 450–462, doi:10.1002/gbc.20039, 2013.

Najjar, R. G., and Orr, J.: Biotic-HOWTO, internal OCMIP report, 15 pp., Lab. des Sci. du Clim. et l’Environ., CEA, Saclay, Gif-sur-Yvette, France, 1999.

© Author(s) 2017. CC BY 4.0 License.

Nakano, H., and Suginohara, N.: Effects of bottom boundary layer parameterization on reproducing deep and bottom waters in a world ocean model, J. Phys. Oceanogr., 32, 1209–1227, 2002.

Oka, A., Abe-Ouchi, A., Chikamoto, M. O., and Ide, T.: Mechanisms controlling export production at the LGM: Effects of changes in oceanic physical field and atmospheric dust deposition, Global Biogeochem. Cycles, 25, GB2009, doi:10.1029/2009GB003628, 2011.

Orr, J. C.: Global Ocean Storage of Anthropogenic Carbon (GOSAC), final report, 117 pp., EC Environ. and Clim. Programme, Inst. Pierre Simon Laplace, Paris, 2002.

Oschlies, A., Schulz, K. G., Riebesell, U., and Schmittner, A.: Simulated 21st century's increase in oceanic suboxia by CO_2-enhanced biotic carbon export, Global Biogeochem. Cycles, 22, GB4008, doi:10.1029/2007GB003147, 2008.

Plattner, G. K., Joos, F., Stocker, T. F., and Marchal, O.: Feedback mechanisms and sensitivities of ocean carbon uptake under global warming, Tellus Ser. B-Chem. Phys. Meteorol., 53(5), 564– 592, 2001.

Plattner, G.-K., Knutti, R., Joos, F., et al.: Long-term climate commitments projected with climate – carbon cycle models, J. Climate, 21, 2721–2751, 2008.

Ridgwell, A., Zondervan, I., Hargreaves, J. C., Bijma, J., and Lenton, T. M.: Assessing the potential long-term increase of oceanic fossil fuel CO_2 uptake due to CO_2-calcification feedback, Biogeosciences, 4, 481–492, 2007.

Riebesell, U., Zondervan, I., Rost, B., Tortell, P. D., Zeebe, R. E., and Morel, F. M. M.: Reduced calcification of marine plankton in response to increased atmospheric CO_2, Nature, 407, 364–367, 2000.

Sarmiento, J. L., Hughes, T., Stouffer, R., and Manabe, S.: Simulated response of the ocean carbon cycle to anthropogenic climate warming, Nature, 393, 245–248, 1998.

Sarmiento, J. L., and Gruber, N.: Ocean Biogeochemical Dynamics, chap. 8, Carbon cycle, pp.318-358, Princeton Univ. Press, Princeton, N. J, 2006.

Schlitzer, R.: Applying the adjoint method for global biogeochemical modeling, in Inverse Methods in Biogeochemical Cycles, edited byP. Kasibhatla et al., pp. 107–124, AGU, Washington, D. C, 2000.

Schmittner, A., Oschlies, A., Matthews, D., and Galbraith, E. D.: Future changes in climate, ocean circulation, ecosystems and biogeochemical cycling simulated for a business-as-usual CO_2 emission scenario until year 4000 AD, Global Biogeochem. Cycles, 22, GB1013, doi:10.1029/2007GB002953, 2008.

Semtner, A. J., Jr.: A model for the thermodynamic growth of sea ice in numerical investigations of climate, J. Phys. Oceanogr., 6, 379–389, 1976.

Smith, S. L., Yamanaka, Y., Pahlow, M., and Oschlies, A.: Optimal uptake kinetics: Physiological acclimation explains the pattern of nitrate uptake by phytoplankton in the ocean, Mar. Ecol. Prog. Ser., 384, 1–12, 2009.

Steinacher, M., Joos, F., Fr¨olicher, T. L., Bopp, L., Cadule, P., Cocco, V., Doney, S. C., Gehlen, M., Lindsay, K., Moore, J. K., Schneider, B., and Segschneider, J.: Projected 21st century decrease in marine productivity: a multi-model analysis, Biogeosciences, 7, 979–1005, doi:10.5194/bg-7-979-2010, 2010.

© Author(s) 2017. CC BY 4.0 License.

Takahashi, T., Olafsson, J., Goddard, J. G., Chipman, D. W., and Sutherland, S. C.: Seasonal variation of CO_2 and nutrients in the high-latitude surface oceans: a comparative study, Global Biogeochem. Cycles, 7, 843-878, 1993.

Taylor, K. E., Stouffer, R. J., and Meehl, G. A.: An overview of CMIP5 and the experiment design, Bull. Am. Meteorol. Soc., 93, 485–498, 2012.

Taucher, J., Bach, L. T., Riebesell, U., and Oschlies, A.: The viscosity effect on marine particle flux: A climate relevant feedback mechanism, Global Biogeochem. Cycles, 28, 415-422, doi10.1002/2013/GB004728, 2014.

Yamamoto, A., Yamanaka, Y., Oka, A., and Abe-Ouchi, A.: Ocean oxygen depletion due to decomposition of submarine methane hydrate, Geophys. Res. Lett., 41, 5075–5083, doi:10.1002/2014GL060483, 2014.

Yamamoto, A., Abe-Ouchi, A., Shigemitsu, M., Oka, A., Takahashi, K., Ohgaito, R., and Yamanaka, Y.: Global deep ocean oxygenation by enhanced ventilation in the Southern Ocean under long-term global warming, Global Biogeochem. Cycles, 29, doi:10.1002/2015GB005181, 2015.

Zickfeld, K., Fyfe, J. C., Saenko, O. A., Eby, M., and Weaver, A. J.: Response of the global carbon cycle to human-induced changes in Southern Hemisphere winds, Geophys. Res. Lett., 34, L12712, doi:10.1029/2006GL028797, 2007.

Zickfeld, K., Eby, M., and Weaver, A. J.: Carbon-cycle feedbacks of changes in the Atlantic meridional overturning circulation under future atmospheric CO_2, Global Biogeochem. Cycles, 22, Gb3024, doi:10.1029/2007GB003118, 2008.

Zickfeld, K., Eby, M., Weaver, A., Alexander, K., Crespin, E., Edwards, N., Eliseev, A., Feulner, G., Fichefet, T., Forest, C., Friedlingstein, P., Goosse, H., Holden, P., Joos, F., Kawamiya, M., Kicklighter, D., Kienert, H., Matsumoto, K., Mokhov, I., Monier, E., Olsen, S., Pedersen, J., Perrette, M., Philippon- Berthier, G., Ridgwell, A., Schlosser, A., Schneider von Deim- ling, T., Shaffer, G., Sokolov, A., Spahni, R., Steinacher, M., Tachiiri, K., Tokos, K., Yoshimori, M., Zeng, N., and Zhao, F.: Long-term climate change commitment and reversibil- ity: An EMIC intercomparison, J. Climate, 26, 5782–5809, doi:10.1175/JCLI-D-12-00584.1, 2013.

Biogeosciences Discuss., https://doi.org/10.5194/bg-2017-451
Manuscript under review for journal Biogeosciences
Discussion started: 10 November 2017
© Author(s) 2017. CC BY 4.0 License.

Figures

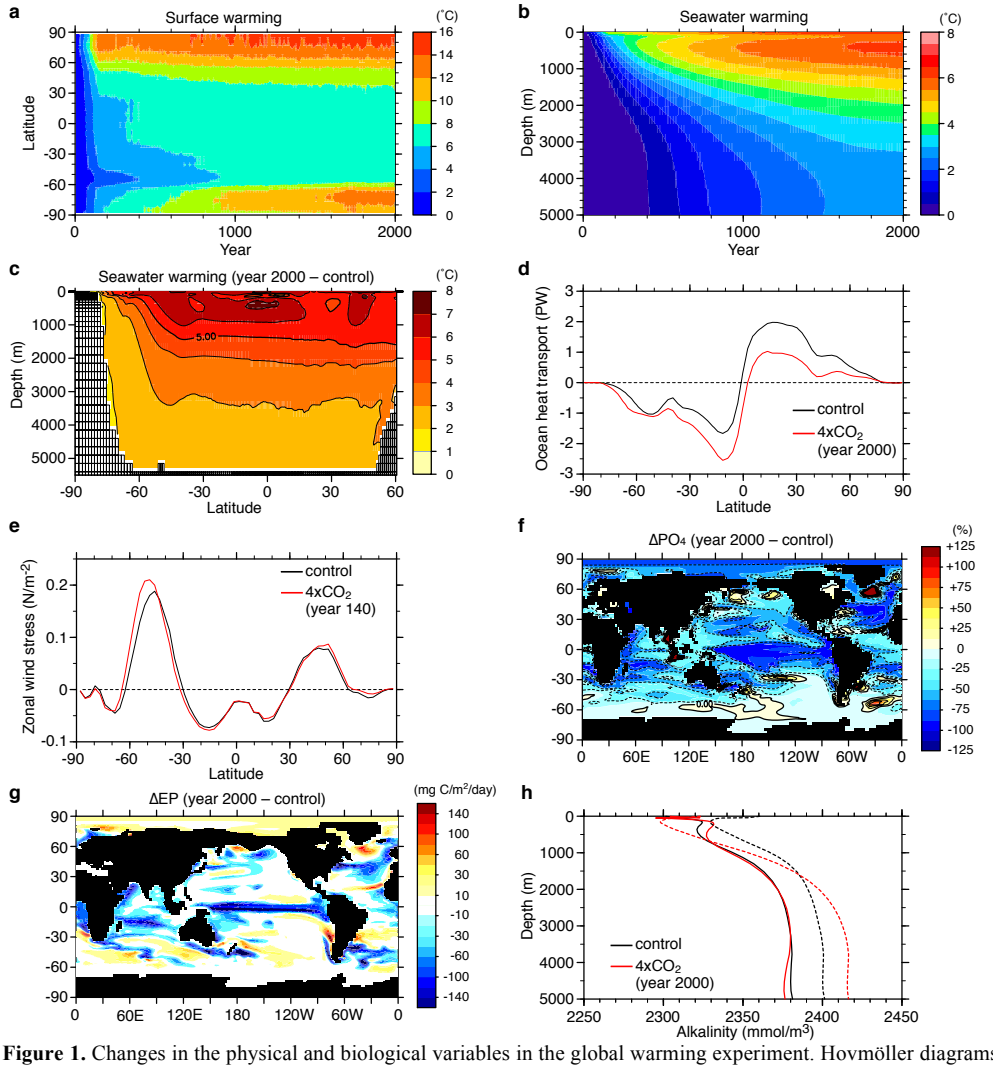

Figure 1. Changes in the physical and biological variables in the global warming experiment. Hovmöller diagrams of (a) the zonally averaged anomaly of the surface temperature and (b) the horizontally averaged anomaly of the seawater temperature. (c) Zonal mean changes in the seawater temperature between the control run and the end of the global warming experiment (year 2000). (d) Northward ocean heat transport for the control (black) and the end of the global warming runs (red). (e) Zonal mean wind stress for the control run (black) and at the time of CO_2 quadrupling (year 140: red). Changes in (f) the surface PO_4 (averaged over the top 50 m) and (g) the export production at the end of the global warming run. Vertical profile

Biogeosciences Discuss., https://doi.org/10.5194/bg-2017-451
Manuscript under review for journal Biogeosciences
Discussion started: 10 November 2017
© Author(s) 2017. CC BY 4.0 License.

of the alkalinity (solid lines) and salinity-normalized alkalinity (dashed lines) for the control (black) and global warming runs (red).

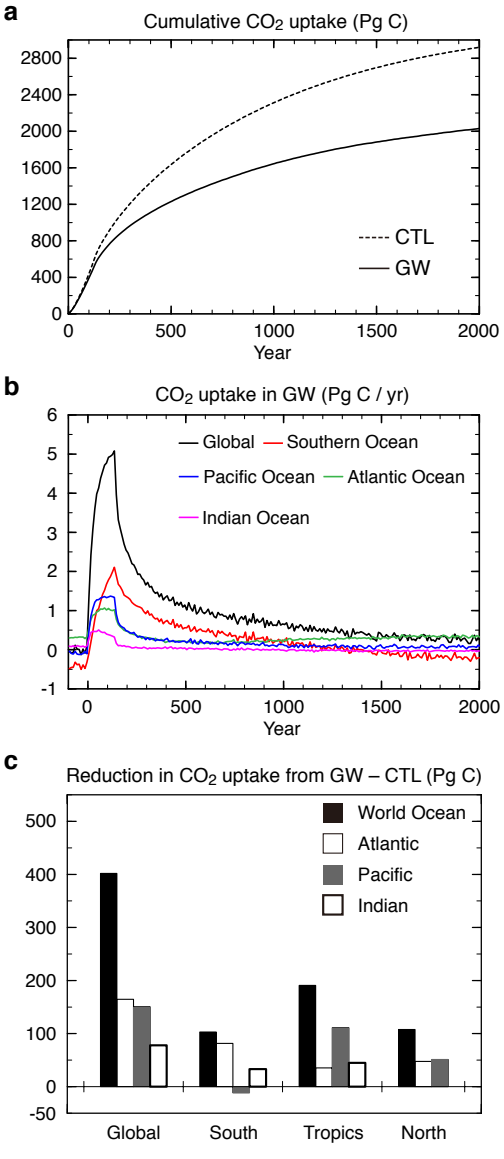

5

Biogeosciences Discuss., https://doi.org/10.5194/bg-2017-451
Manuscript under review for journal Biogeosciences
Discussion started: 10 November 2017
© Author(s) 2017. CC BY 4.0 License.

Figure 2. (a) Time series of the cumulative oceanic CO_2 uptake for CTL (dashed line) and GW (solid line). (b) Time series of the annual mean values of the oceanic CO_2 uptake for the global ocean (black) and different ocean basins (colors) in GW. (c) Reduction in the oceanic CO_2 uptake due to global warming for the global ocean and three ocean basins at 500 years (GW–CTL). The contributions of the global ocean and individual ocean basins are separated into three regions (South: south of 32.5°S; tropics: 32.5°S–32.5°N; north: north of 32.5°N). The positive and negative values represent uptake reductions and uptake increases, respectively.

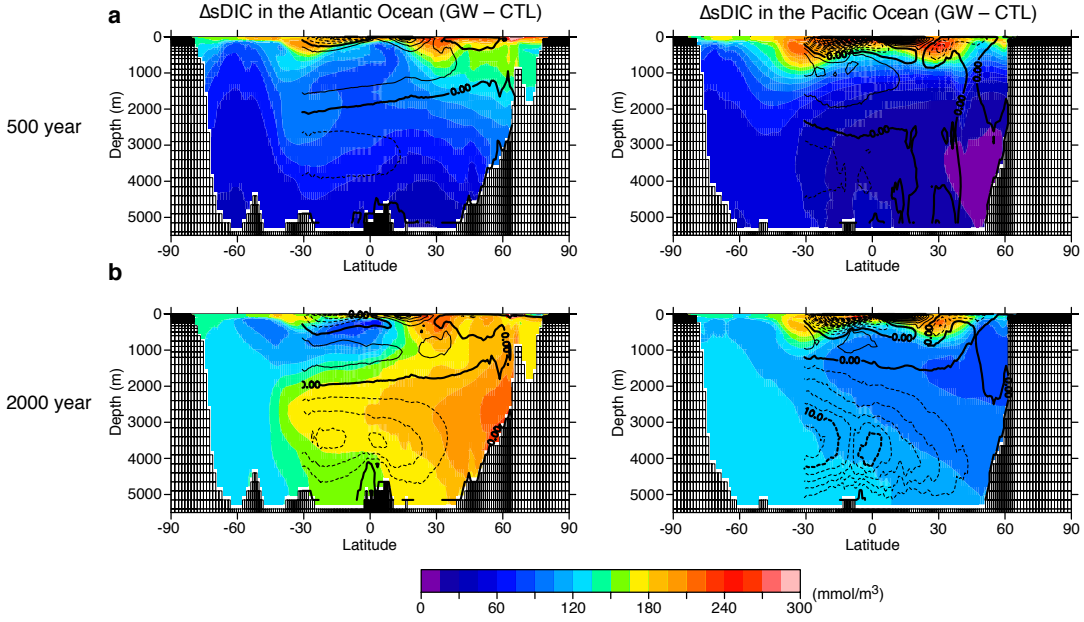

Figure 3. Zonal mean distribution of changes in the salinity-normalized DIC (colors) and meridional overturning stream function (contours) for (a) 500 years and (b) 2000 years in the global warming run (GW). The left and right panels show the Atlantic and Indo-Pacific Oceans, respectively. The contour interval is 2 Sv.

Biogeosciences Discuss., https://doi.org/10.5194/bg-2017-451
Manuscript under review for journal Biogeosciences
Discussion started: 10 November 2017
© Author(s) 2017. CC BY 4.0 License.

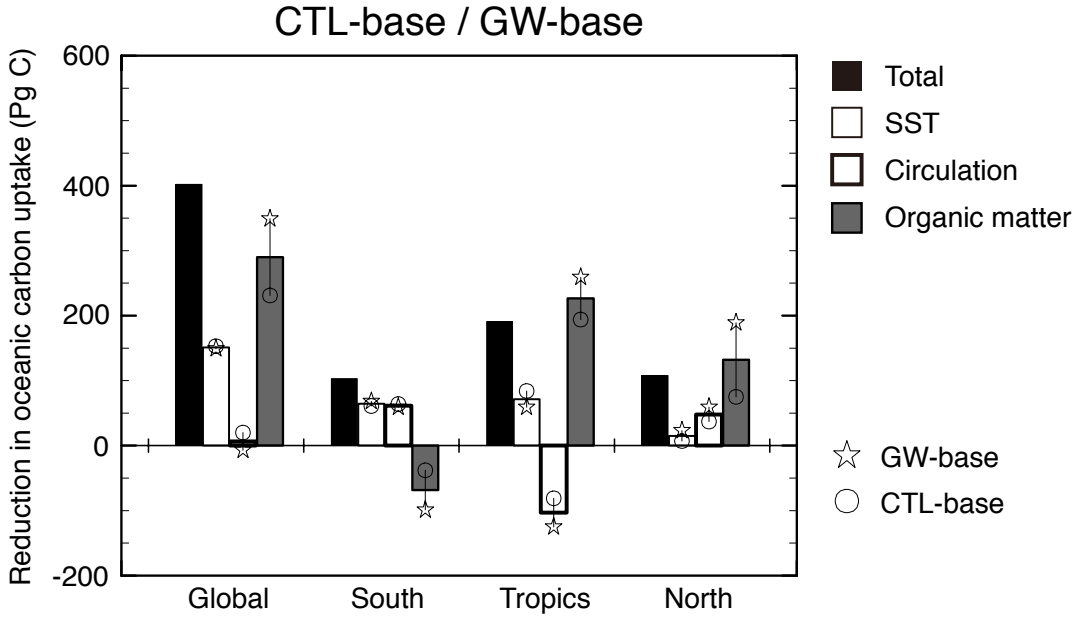

Figure 4. Contributions of the primary mechanisms to the reduction in the oceanic CO_2 uptake due to global warming at 500 years for the CTL-base/GW-base experiments. The total change and the effects of SST, circulation, and organic matter are calculated as summarized in Table 2. The contributions of the individual mechanisms are separated into three regions (South: south of 32.5°S; tropics: 32.5°S–32.5°N; north: north of 32.5°N). The bars refer to the averages of CTL-base and GW-base.

Biogeosciences Discuss., https://doi.org/10.5194/bg-2017-451
Manuscript under review for journal Biogeosciences
Discussion started: 10 November 2017
© Author(s) 2017. CC BY 4.0 License.

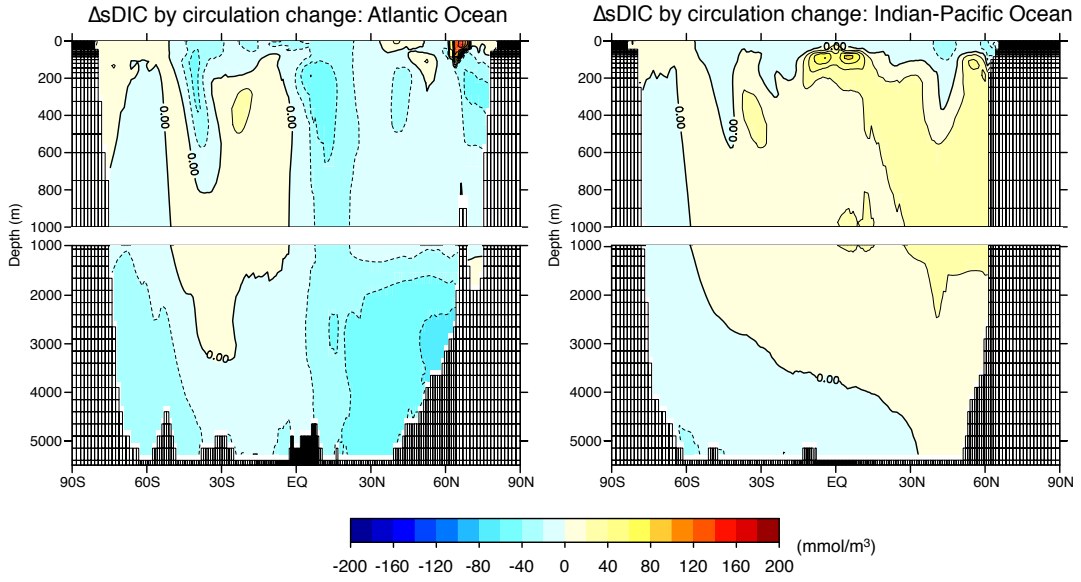

Figure 5. Zonal mean changes in the salinity-normalized DIC induced by circulation changes for the CTL-base/GW-base experiments at 500 years. The left and right panels show the Atlantic and Indo-Pacific Oceans, respectively.

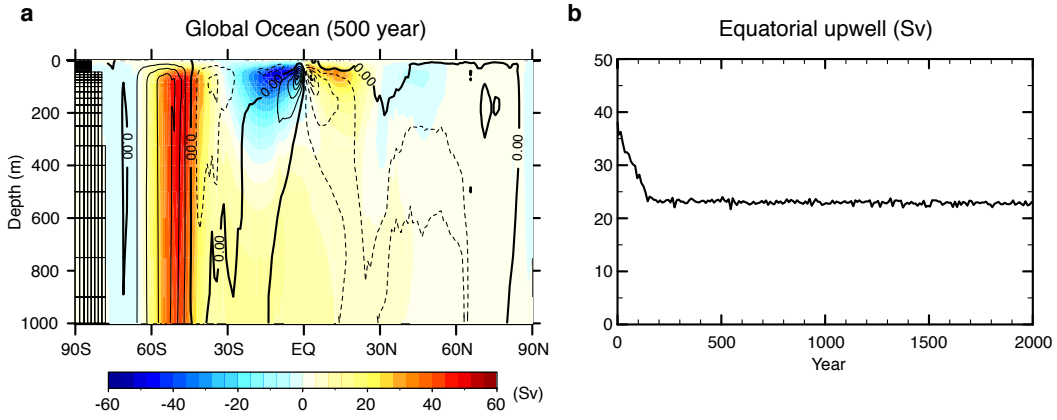

Figure 6. Global upper-ocena overturning circulation. (a) Meridional overturning stream function at year 500 (colors). The positive numbers represent clockwise circulation, and the negative numbers represent counterclockwise circulation. The contours show the differences between meridional overturning stream function in year 500 and the pre-industrial condition. The contour interval is 4 Sv. (b) Time series of global equatorial upwelling (through 200m, between 10˚S and 10˚N)

Biogeosciences Discuss., https://doi.org/10.5194/bg-2017-451
Manuscript under review for journal Biogeosciences
Discussion started: 10 November 2017
© Author(s) 2017. CC BY 4.0 License.

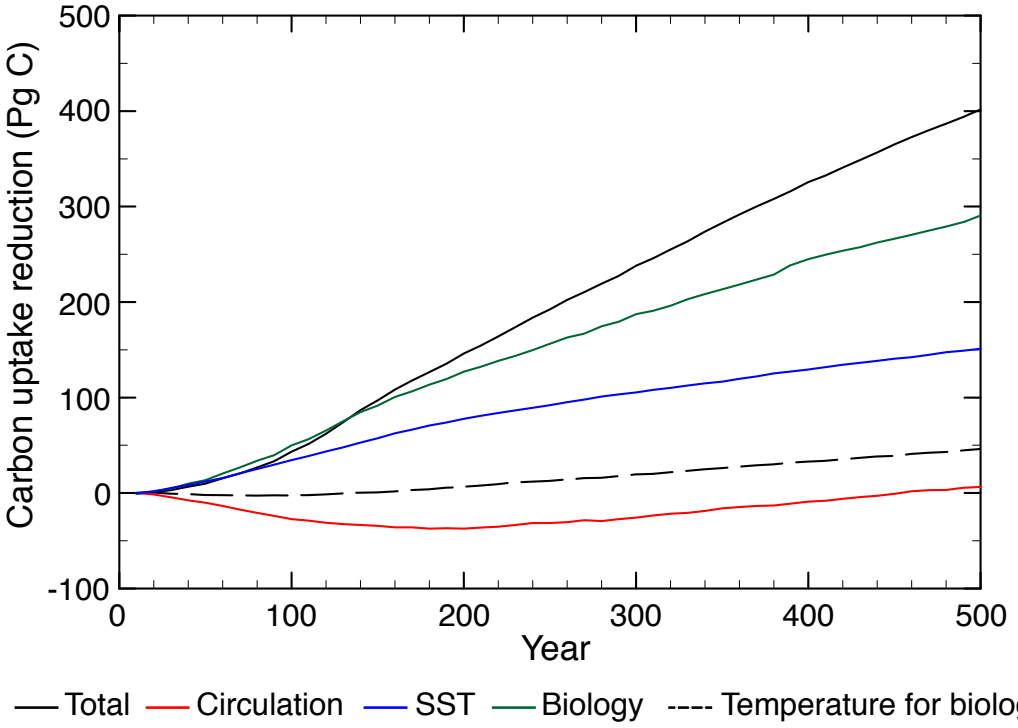

Figure 7. Time series of the contributions of the primary mechanisms to the reduction in the oceanic CO_2 uptake in the CTL-base/GW-base experiments. The positive and negative values represent uptake increases and decreases, respectively. The contributions of circulation (red), biology (green), and SST (blue) and the temperature dependences of production and remineralization (black dashed line) are illustrated. The methods for the quantification of each mechanism are summarized in Table 2.

Biogeosciences Discuss., https://doi.org/10.5194/bg-2017-451
Manuscript under review for journal Biogeosciences
Discussion started: 10 November 2017
© Author(s) 2017. CC BY 4.0 License.

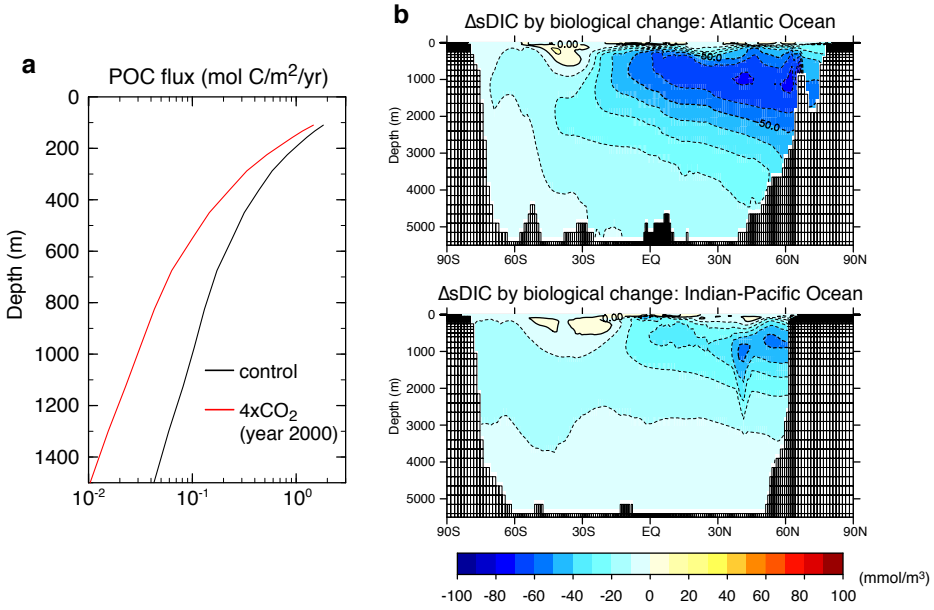

Figure 8. Contribution of the reorganization of the organic matter cycle. (a) Vertical distribution of the POC flux for the control (black) and global warming runs (red). (b) Zonal mean changes in the salinity-normalized DIC induced by changes in the organic matter cycle in the CTL-base/GW-base experiments at 500 years. The top and bottom panels show the Atlantic and Indo-Pacific Oceans, respectively.

Biogeosciences Discuss., https://doi.org/10.5194/bg-2017-451
Manuscript under review for journal Biogeosciences
Discussion started: 10 November 2017
© Author(s) 2017. CC BY 4.0 License.

	Experiments	Changing mechanisms	Cumulative uptake (Pg C) 500year	2000year	SST	Dilution	Circulation	Organic matter cycle	$CaCO_3$ cycle	Sea ice
1	CTL	–	1629	2888	CTL	CTL	CTL	CTL	CTL	CTL
2	GW	all	1227	2028	GW	GW	GW	GW	GW	GW
3	GW_SST	SST	1376		CTL	GW	GW	GW	GW	GW
4	GW_fw	freshwater flux	1230		GW	CTL	GW	GW	GW	GW
5	GW_circ	circulation	1220		GW	GW	CLT	GW	GW	GW
6	GW_om	organic matter cycle	1563		GW	GW	GW	CTL	GW	GW
7	GW_ca	CaCO3cycle	1240		GW	GW	GW	GW	CTL	GW
8	GW_si	sea ice	1211		GW	GW	GW	GW	GW	CTL
9	GW_biotemp	temperature for biology	1278		GW	GW	GW	GW*	GW*	GW
10	CTL_SST	SST	1476		GW	CTL	CTL	CTL	CTL	CTL
11	CTL_fw	freshwater flux	1627		CTL	GW	CTL	CTL	CTL	CTL
12	CTL_circ	circulation	1609		CTL	CTL	GW	CTL	CTL	CTL
13	CTL_om	organic matter cycle	1413		CTL	CTL	CTL	GW	CTL	CTL
14	CTL_ca	CaCO3cycle	1614		CTL	CTL	CTL	CTL	GW	CTL
15	CTL_si	sea ice	1643		CTL	CTL	CTL	CTL	CTL	GW
16	CTL_biotemp	temperature for biology	1583		CTL	CTL	CTL	CTL**	CTL**	CTL

*Pre-industrial seawater temperature is used for calculating biological term in GW_biotemp.

**Seawater temperature of GW_bio is applied for calculating biological term in CTL_biotemp.

Table 1: Description of the model experiments and results of the oceanic CO_2 uptake.

Biogeosciences Discuss., https://doi.org/10.5194/bg-2017-451
Manuscript under review for journal Biogeosciences
Discussion started: 10 November 2017
© Author(s) 2017. CC BY 4.0 License.

Mechanisms	GW-base	uptake change (Pg C)	CTL- base	uptake change (Pg C)	average of GW-base and CTL-base (Pg C)
Total	(2) − (1)	-402	(2) − (1)	-402	-402
SST	(2) − (3)	-149	(10) − (1)	-153	-151
Freshwater	(2) − (4)	-3	(11) − (1)	-2	-2.5
Circulation	(2) − (5)	7	(12) − (1)	-20	-6.5
Sea ice	(2) − (8)	16	(15) − (1)	14	15
Biology	(Organic matter cycle) + ($CaCO_3$ cycle)	-349	(Organic matter cycle) + ($CaCO_3$ cycle)	-231	-290
Organic matter cycle	(2) − (6)	-336	(13) − (1)	-216	-276
$CaCO_3$ cycle	(2) − (7)	-13	(14) − (1)	-15	-14
Temperature for biology	(2) − (9)	-51	(16) − (1)	-46	-48.5
Nutrient supply	(Biology) − (Temperature for biology)	-298	(Biology) − (Temperature for biology)	-185	-241.5
residual		76		-10	33

Table 2: The contributions of individual mechanisms to the reduction in the CO_2 uptake due to global warming in the first 500 years.